0090-9556/06/3410-1688–1696$20.00
DRUG METABOLISM AND DISPOSITION
Vol. 34, No. 10
10678/3137982
DMD 34:1688–1696, 2006
Printed in U.S.A.

Amiodarone Analog-Dependent Effects on CYP2C9-Mediated Metabolism and Kinetic Profiles

Vikas Kumar, Chuck W. Locuson, Yuk Y. Sham, and Timothy S. Tracy

Department of Experimental and Clinical Pharmacology, University of Minnesota, Minneapolis, Minnesota (V.K, C.W.L., T.S.T.); and University of Minnesota Supercomputing Institute, Minneapolis, Minnesota (Y.Y.S.)

Received April 19, 2006; accepted June 27, 2006

ABSTRACT:

CYP2C9 substrates can exhibit both hyperbolic and atypical kinetic profiles, and their metabolism can be activated or inhibited depending on the effector studied. CYP2C9 genetic variants can also affect both substrate turnover and kinetic profile. The present study assessed whether analogs of the effector amiodarone differentially altered the atypical kinetic profile of the substrate naproxen and whether this effect was genotype-dependent. Amiodarone, desethylamiodarone, benzbromarone, and its dimethyl analog (benz(meth)arone) were incubated with naproxen and either CYP2C9.1 or CYP2C9.3. Amiodarone activated naproxen demethylation at lower concentrations, regardless of the CYP2C9 allele, and inhibited metabolism at higher concentrations without altering the kinetic profile. Desethylamiodarone was a potent inhibitor of naproxen demethylation, irrespective of the CYP2C9 allele. Benzbromarone altered naproxen demethylation kinetics from a biphasic profile to that of a hyperbolic form in CYP2C9.1 and CYP2C9.3, resulting in inhibition and activation, respectively. In contrast, benz(meth)arone activated naproxen demethylation in both CYP2C9.1 and CYP2C9.3. In addition, the kinetic profile of naproxen demethylation became more hyperbolic at lower concentrations of benz(meth)arone and then reverted back to biphasic as the benz(meth)arone was increased further. Equilibrium binding and multiple-ligand docking studies were used to propose how such similar compounds exerted very different effects on naproxen metabolism. In summary, effectors of CYP2C9 metabolism can alter not only the degree of substrate turnover (activation or inhibition) but also the kinetic profile of metabolism of CYP2C9 substrates through effects on substrate binding and orientation. In addition, these kinetics effects are concentration- and genotype-dependent.

The cytochrome P450 family of enzymes is involved in the oxidative metabolism of drugs and xenobiotics. Cytochrome P450 2C9 (CYP2C9) is a member of this enzyme family and has been estimated to be responsible for the metabolism of about 20% of marketed drugs (Rendic and Di Carlo, 1997). CYP2C9 exhibits genetic polymorphisms, and 24 variant alleles of CYP2C9 have been discovered to date (http://www.imm.ki.SE/CYPalleles/). One of these variants, CYP2C9.3, is observed frequently in the white (not Hispanic) population (~10–15% allele frequency) (Lee et al., 2002) and has been the subject of many studies. The CYP2C9.3 variant substantially affects turnover for some substrates as evidenced by reductions in V_m of 50 to 90% compared with the wild-type enzyme. Furthermore, the K_m of the substrate can be increased severalfold in the CYP2C9.3 variant compared with wild-type enzyme, but again, the magnitude of these effects is substrate-dependent. These alterations in V_m and K_m, therefore, also affect the intrinsic clearance (V_m/K_m) for this enzyme. For example, Takanashi et al. (2000) studied the effect of CYP2C9 variants on the V_m/K_m ratio for seven CYP2C9 substrates (diclofenac, warfarin, tolbutamide, tenoxicam, piroxicam, phenytoin, and mefenamic acid) and found that the V_m/K_m values were 3.4- to 26.9-fold lower in expressed CYP2C9.3 compared with CYP2C9.1. These reductions in V_m/K_m can necessitate dosage adjustments in individuals on narrow therapeutic index drugs such as warfarin and phenytoin (Higashi et al., 2002; Tate et al., 2005).

Desethylamiodarone, a metabolite of amiodarone, has been observed to be a potent inhibitor of CYP2C9-mediated warfarin hydroxylation (K_i = 2.3 μM) both in vitro and in vivo (Ohyama et al., 2000), whereas coadministration of amiodarone only resulted in weak inhibition of CYP2C9. In contrast, in CYP2C9.1, in vitro activation of 7-methoxy-4-trifluoromethyl-coumarin and naproxen demethylation by amiodarone have been reported (Egnell et al., 2003; McGinnity et al., 2005), suggesting that the type of effect observed (inhibition versus activation) may be analog- and substrate-dependent. Similarly, benzbromarone (BZBR) and its analogs are some of the most potent inhibitors of CYP2C9 described to date. Locuson et al. (2004) studied the inhibition potential of BZBR and its dimethyl analog (benz(meth)arone) in CYP2C9.1 with warfarin and reported that these two compounds strongly inhibited warfarin 7-hydroxylation, exhibiting K_i values of 19 nM and 40 nM, respectively. More recently, pharmacogenetic differences in the effect of BZBR on flurbiprofen kinetics have been reported in the CYP2C9.3 allele compared with wild-type CYP2C9 (Hummel et al., 2005). BZBR inhibited the metabolism of flurbiprofen by CYP2C9.1, whereas an opposite effect (i.e., activa-

Funded in part by Grants GM063215 and GM069753 from the National Institutes of Health.

Article, publication date, and citation information can be found at http://dmd.aspetjournals.org.

doi:10.1124/dmd.106.010678.

ABBREVIATIONS: BZBR, benzbromarone; P450, cytochrome P450; CPR, cytochrome P450 reductase; benz(meth)arone, ((2-ethylbenzofuran-3-yl)-(4-hydroxy-3,5-dimethylphenyl)methanone); HPLC, high-performance liquid chromatography.

tion) was observed when its effects on flurbiprofen metabolism were studied with CYP2C9.3. However, this study only addressed a single effector agent (BZBR), whereas the studies mentioned above suggest that analogs of amiodarone, possessing different physicochemical properties, may have differing effects on metabolism (e.g., inhibition versus activation). In addition, no studies have addressed this question with other analogs of amiodarone, and variants of CYP2C9.

When examined together, results of the aforementioned studies suggest that substrate, effector, and genotype may need to be considered when assessing both degree and type of in vitro drug-drug interactions. To this end, the present study was designed to evaluate the structure-activity relationships of four amiodarone analogs on the metabolism of a substrate exhibiting atypical biphasic kinetics, naproxen (Korzekwa et al., 1998), in both CYP2C9.1 and CYP2C9.3. These studies address whether effector-dependent alterations in the kinetic profile of this atypical kinetics compound occur and whether the alterations in kinetic profile are genotype-dependent. Observed changes in kinetic profile due to different analogs of amiodarone were correlated with docking energies to discern possible mechanisms for the observed effects.

Materials and Methods

Chemicals. Acetonitrile, potassium phosphate, glycerol, and EDTA were purchased from Fisher Scientific (Pittsburgh, PA). NADPH, dilauroylphosphatidylcholine (DLPC), amiodarone, and BZBR were obtained from Sigma (St. Louis, MO). (*S*)-Naproxen and desmethylnaproxen were gifts from the former Syntex Laboratories (Palo Alto, CA). The internal standard used was 2-fluoro 4-biphenyl acetic acid and was a gift from the former Pharmacia Co. (Kalamazoo, MI). Desethylamiodarone was a gift from Dr. Mark Reasor (West Virginia University, Morgantown, WV) and (2-ethylbenzofuran-3-yl)-(4-hydroxy-3,5-dimethylphenyl)methanone) (abbreviated as benz(meth)arone) was a gift from Dr. Jeffery P. Jones at Washington State University (Pullman, WA). Human cytochrome b_5 was purchased from Invitrogen, Inc. (Carlsbad, CA). All other chemicals used were obtained from commercial sources and were of the highest purity available.

Cytochrome P450 2C9 and Cytochrome P450 Reductase (CPR) Expression. Cytochrome P450 2C9.1 and 2C9.3 were expressed and purified as described previously (Hummel et al., 2005). Rat CPR was expressed and purified according to the methods described by Hanna et al. (1998). The pOR263 plasmid containing the rat P450 reductase gene was obtained from Dr. Paul Hollenberg at the University of Michigan (Ann Arbor, MI).

In Vitro Incubation Conditions. Metabolic incubations were carried out according to the methods of Tracy et al. (1997) with slight modification. Incubation mixtures contained 5 to 20 pmol of purified P450, CPR, and cytochrome b_5 in a 1:2:1 ratio, reconstituted with DLPC vesicles extruded through a 200-nm pore-sized membrane. To study the effects of amiodarone and its analogs (Fig. 1) on CYP2C9.1- and CYP2C9.3-mediated naproxen demethylation, nine concentrations of (*S*)-naproxen, 10 to 900 μM, were incubated with four concentrations (0–500 μM and 0–10 μM) each of amiodarone and desethylamiodarone, respectively; seven concentrations (0–3200 nM) of BZBR; and nine concentrations (0–6400 nM) of benz(meth)arone. To further characterize the effect of amiodarone on naproxen demethylation, more extensive kinetic studies were conducted with nine concentrations of amiodarone (0–500 μM) at a single concentration (300 μM) of naproxen. Organic solvents (except benzbromarone, which was dissolved in potassium phosphate buffer) used to dissolve amiodarone (dimethyl sulfoxide) and its analogs (desethylamiodarone in ethanol and benz(meth)arone in methanol) were kept constant in test as well as control incubations, and the final concentration of the solvent was lower than 2.5%. All incubations were conducted for 20 min at 37°C in 50 mM potassium phosphate buffer, pH 7.4, in a final volume of 200 μl. After a 3-min preincubation, reactions were initiated by the addition of NADPH (1 mM final concentration). Reactions were quenched by the addition of 200 μl of acetonitrile containing internal standard, 180 ng/ml 2-fluoro-4-biphenylacetic acid. After quenching, 40 μl of H_3PO_4 (7.6 M) was added to the reaction mixtures. Samples were then centrifuged at 10,600*g* for 4 min, placed into autosampler vials, and 50 μl was injected onto the HPLC system.

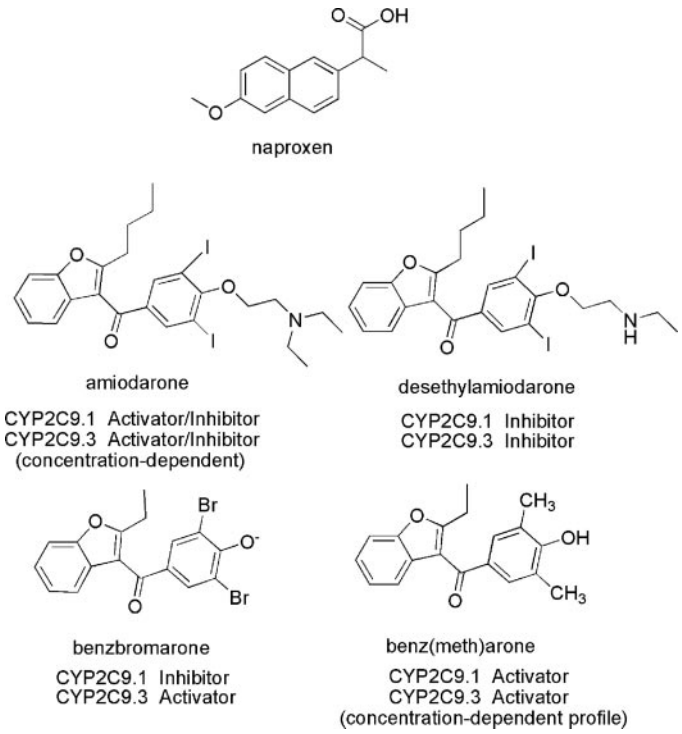

FIG. 1. Structure of amiodarone analogs and their differing effects on the in vitro metabolism of substrate naproxen.

Quantitation of Desmethylnaproxen. HPLC analysis of desmethylnaproxen production was conducted as described previously (Tracy et al., 1997). The HPLC system consisted of a Waters Alliance 2695XE chromatographic system (Waters, Milford, MA) and a Waters model 2475 fluorescence detector. The mobile phase was pumped through a Brownlee Spheri-5 C_{18} 4.6 mm × 100 mm column at 1 ml/min. For quantification of desmethylnaproxen, the detector was set at an excitation wavelength of 230 nm and an emission wavelength of 340 nm, which switched to an excitation wavelength of 260 nm and an emission wavelength of 320 nm after 4 min for detection of internal standard. The mobile phase consisted of 40:60 acetonitrile/20 mM potassium phosphate, pH 3.0. The retention times for desmethylnaproxen and the internal standard were approximately 1.9 and 6.8 min, respectively.

Kinetic Data Analysis. The formation of desmethylnaproxen from the parent compound naproxen was fit according to eq. 1 (Korzekwa et al., 1998). The following equation describes a biphasic kinetic model in which two substrate molecules bind simultaneously to different regions of the enzyme:

$$v = \frac{(V_{m1} \cdot [S]) + (CL_{int}) \cdot [S]^2}{(K_{m1} + [S])} \quad (1)$$

where S is substrate concentration, V_{m1} and K_{m1} are estimated kinetic constants for the curved portion of the graph at lower concentrations, and CL_{int} (intrinsic clearance) is the slope of the linear portion of the graph at higher concentrations.

Inhibition and activation kinetics parameters were estimated with the following equations. A biphasic competitive inhibition model (eq. 2) was used to determine the K_i value for amiodarone, desethylamiodarone, and BZBR in CYP2C9.1,

$$v = \frac{(V_{m1} \cdot [S]) + (CL_{int}) \cdot [S]^2}{((1 + I/K_i) K_{m1} + [S])} \quad (2)$$

where I is inhibitor concentration and K_i is inhibition constant, and the remaining parameters are as defined above.

A biphasic activation model (eq. 3) was used to determine K_a, α,

and β values for benz(meth)arone in both CYP2C9.1 and CYP2C9.3 and also to determine these parameters for BZBR in CYP2C9.3.

$$\nu = \frac{(V_{m1} \cdot [S]) + (CL_{int}) \cdot [S]^2}{\left(\frac{K_{m1}(1 + [A]/K_a)}{1 + \beta[A]/\alpha[A]}\right) + \left(\frac{[S](1 + [A]/\alpha K_a)}{1 + \beta[A]/\alpha K_a}\right)} \quad (3)$$

In the above equation, A is activator concentration, K_a is the binding constant of the activator, and α and β are the interaction terms reflecting effects on K_{m1} and V_{m1} in the presence of activator.

A linear equation (eq. 4) was used to determine intrinsic clearance of naproxen at different concentrations of amiodarone and desethylamiodarone in CYP2C9.3.

$$\nu = (CL_{int}) \cdot [S] \quad (4)$$

All the data were fit with Sigma Plot 8.0 (Systat Software, Point Richmond, CA) and the goodness of the fit was determined by examination of the residuals, residual sum of squares, coefficients of determination, and F values.

Equilibrium Substrate Binding. Binding of (*S*)-naproxen was monitored by its ability to alter the spin state of the heme iron via rearrangement of active site water(s). Experiments were conducted with a dual-beam spectrophotometer (Aminco DW-2000 upgrade; Olis, Inc., Bogart, GA) with wavelengths scanned from 340 to 500 nm over both an enzyme-containing solution in the sample cuvette and the reference cuvette, which contained only buffer. By titrating (*S*)-naproxen into both cuvettes, the large naproxen signal evident at higher concentrations was essentially subtracted out. Titration of 5 to 1000 μM (*S*)-naproxen into 0.5 μM CYP2C9/1.0 μM CPR/0.5 μM cytochrome b_5 in 50 mM potassium phosphate buffer, pH 7.4, demonstrated that naproxen induces an increase in the fraction of high-spin iron P450 and a concomitant decrease in low-spin P450 species (also known as type I binding interaction). The difference in peak height of the high-spin (390 nm) and low-spin (418 nm) spectral components was used as the spectroscopic signal for binding analysis, although comparable values could be obtained from the low-spin peak area. Spectral dissociation constants (K_S) were measured for (*S*)-naproxen both in the absence and presence of benz(meth)arone, either equimolar to CYP2C9 or in 10-fold excess. At equimolar concentrations, benz(meth)arone did not induce any detectable change in P450 spin state, but at a concentration of 5.0 μM, benz(meth)arone generated ~55% of the signal amplitude achievable with 1000 μM naproxen alone. This signal did not interfere with the subsequent titration of naproxen, since it only altered the initial absorbance values. Because it was not possible to fully saturate the enzyme with naproxen and because the biphasic response suggested that multiple binding events were detectable, K_S values were estimated from the nonlinear regression fits of the two-ligand model:

$$Y = \frac{B_{max1} \cdot S}{K_{S1} + S} + \frac{B_{max2} \cdot S}{K_{S2} + S} \quad (5)$$

where K_{S1} is a saturable, low-K_S site. K_{S2} is a nonsaturable site that may have proximity to the heme such that a bound naproxen ligand can influence spin state. Alternatively, occupation of the K_{S2} site may act indirectly to alter active site solvation or by allowing one naproxen to influence the proximity of a second naproxen to the heme.

A titration with desethylamiodarone alone, at 5 to 35 μM, was carried out in a manner similar to that with CYP2C9, except that difference spectra were collected and CPR and cytochrome b_5 were omitted.

Substrate and Effector Docking. The program Glide v3.5 (Schrodinger, LLC, Portland, OR) was used to determine the most favorable binding orientations for naproxen and the amiodarone analogs. Two forms of the 1R9O crystal structure (Wester et al., 2004) were used in docking studies because this structure was cocrystallized with the nonsteroidal anti-inflammatory (*S*)-flurbiprofen ligand, which is very similar to (*S*)-naproxen. Because the original structure had regions that lacked diffraction data, some modification of the original 1R9O crystal structure was carried out as described previously (Locuson et al., 2006). The Schrodinger suite of molecular modeling software was then used to generate the CYP2C9 receptor from structures that had been equilibrated with both naproxen and benzbromarone or naproxen and benz(meth)arone using molecular dynamics simulations. After adjusting the bond order of the heme prosthetic group, the heme iron was designated to be in the resting ferric (Fe^{3+}) state and the proximal cysteine ligand was given a charge of −1. Hydrogens were added and minimization was carried out until the rmsd changed less than 0.3 Å. Default values were used for cutoff, neutralization, and scaling parameters. A 14-Å box was used to define the range over which the midpoint of the ligand could be placed to search for optimal binding sites. Ligands were generated using AM1 calculations to generate partial charges and starting geometry. The standard precision mode of docking was used with the default number of generated ligand conformations, and the top 10 scoring conformations were saved for analysis. (*S*)-Naproxen, BZBR, benz(meth)arone, amiodarone, and desethylamiodarone were all docked alone, and BZBR, benz(meth)arone, and a second naproxen ligand were additionally docked in the presence of a docked (*S*)-naproxen molecule. After docking of two ligands, further CYP2C9 receptors could be generated so that each binding site in the enzyme could be evaluated with alternate binding modes for naproxen and effectors.

GlideScores were used to evaluate binding of all ligands. The GlideScore is an estimation of ΔG_{bind}, which is acquired with a force field that includes terms for lipophilic, van der Waals, hydrogen bonding, and Coulomb energies, is sensitive to the formal charge of the ligand and receptor, and incorporates explicit solvent molecules to account for solvation energies.

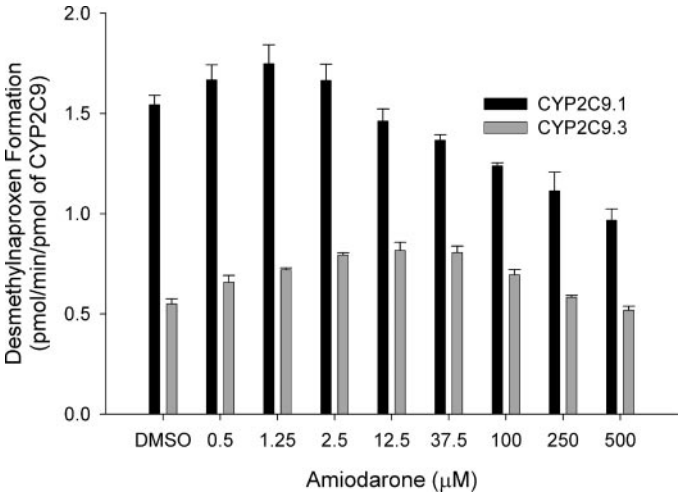

FIG. 2. Desmethylnaproxen formation in the presence of various concentrations of amiodarone when coincubated with 300 μM naproxen using CYP2C9.1 and CYP2C9.3. Each data point is the mean of triplicate determinations.

Results

Amiodarone and the analogs desethylamiodarone, benzbromarone, and benz(meth)arone (Fig. 1) were studied as to their effects on the kinetics of naproxen demethylation with CYP2C9.1 and CYP2C9.3. The effects of amiodarone on the demethylation of naproxen in CYP2C9.1 and CYP2C9.3 are shown in Fig. 2. Amiodarone exhibited no consistent effect on the rate of naproxen demethylation. At low concentrations (<1 μM), it produced weak activation of naproxen demethylation in CYP2C9.1. As the amiodarone concentration was increased above 1.25 μM in CYP2C9.1, this activation was reversed and, eventually, inhibition (amiodarone concentrations >12.5 μM) was noted compared with the control. However, a somewhat different pattern was noted when amiodarone was incubated with naproxen in the CYP2C9.3 enzyme. A more substantial activation of naproxen demethylation was noted in the CYP2C9.3 enzyme, reaching almost 60% activation at 37.5 μM amiodarone. As the concentration of amiodarone was increased further, a reversal of activation was noted

TABLE 1

Kinetic parameter estimates for naproxen demethylation in the presence of various amiodarone analogs

Values represent the mean (standard error of the parameter estimate).

Effector	CYP2C9.1							CYP2C9.3				
	V_{max}	K_m	K_i	K_a	α	β	CL_{int}	V_{max}	K_m	K_a	α	β	CL_{int}
	pmol/min/pmol P450		*μM*					*pmol/min/pmol P450*		*μM*			
Amiodarone[a]	2.2 (0.37)	364 (81)	377 (52)				0.0013						
Benzbromarone	3.45[a] (0.9)	130[a] (61)	0.48[a] (0.26)				0.0012	2.37[b] (0.4)	251[b] (71)	0.27[b] (0.06)	0.52[b] (0.15)	5.05[b] (0.73)	0.0001
Desethylamiodarone[a]	6.2 (1.36)	457 (137)	4.32 (0.74)				0.0011						
Benz(meth)arone[b]	4.6 (0.64)	140 (40)		0.11 (0.03)	1.2 (0.34)	2.3 (0.22)	0.0003	1.06 (0.19)	144 (44)	0.25 (0.07)	0.98 (0.32)	6.82 (0.96)	0.0006

[a] Data were fit to the biphasic competitive inhibition model equation (eq. 2). [It is possible that other types of inhibition may have been present, but due to the complexity of the kinetic processes occurring (biphasic metabolism kinetics overlaid with potentially competitive, mixed, or uncompetitive inhibition) and the amount of data required to describe more complex types of inhibition, the simpler biphasic competitive inhibition equation was used.]

[b] Data were fit to a biphasic activation model (eq. 3).

FIG. 3. Two-site model nonlinear regression fit (eq. 1) of the data for desethylamiodarone inhibition of CYP2C9.1- and CYP2C9.3-mediated naproxen demethylation. Data points represent mean of duplicate determinations.

beginning at 100 μM amiodarone, and eventually, a slight inhibition of naproxen demethylation relative to control was noted at 500 μM amiodarone in CYP2C9.3. Amiodarone had no effect on the kinetic profile of CYP2C9.1- and CYP2C9.3-mediated naproxen demethylation. CYP2C9.1 data were best fit (R^2 = 0.99) to a biphasic competitive inhibition model (eq. 2 and the kinetic parameter estimates are listed in Table 1); CYP2C9.3 data were best fit with a linear equation (eq. 4). Intrinsic clearance increased from 0.0013 to 0.0017 ml/min/pmol CYP2C9.3 when 100 μM amiodarone was added and then decreased to 0.0012 ml/min/pmol CYP2C9.3 at 500 μM amiodarone. These intrinsic clearance values correlate well with the activation and inhibition obtained with different concentrations of amiodarone at 300 μM naproxen in CYP2C9.3, as shown in Fig. 2. To determine whether nonspecific binding of amiodarone to the DLPC vesicles might influence the results observed, an experiment was conducted with three different concentrations of DLPC (5, 10, and 20 μg/incubation) and with four increasing concentrations of amiodarone. At all DLPC concentrations, a similar trend of activation and then inhibition at similar percentages of change compared with control values were noted, suggesting that DLPC concentration had no effect on the amiodarone-mediated alterations in desmethylnaproxen formation (data not shown).

In contrast, desethylamiodarone, the deethylation metabolite of amiodarone, was a potent inhibitor of naproxen demethylation at all concentrations in both CYP2C9.1 and CYP2C9.3 enzymes (Fig. 3). Again, CYP2C9.1 data were best fit (R^2 = 0.99) to a biphasic competitive inhibition model (kinetic parameter estimates for the fit are presented in Table 1), and CYP2C9.3 data were best fit with a linear equation. Intrinsic clearance values for CYP2C9.3 were reduced by half from 0.0018 to 0.0009 with increasing concentrations of desethylamiodarone. This finding suggests that there is little difference in the inhibition potential of desethylamiodarone toward naproxen demethylation, irrespective of the CYP2C9 variant. It is of note that no change in the kinetic profile of naproxen demethylation was observed in either CYP2C9.1 or CYP2C9.3 during coincubation with desethylamiodarone (Fig. 3).

Figure 4, A and B, depicts the effects of BZBR on naproxen demethylation in these two variants of CYP2C9. With CYP2C9.1, BZBR appears to inhibit the metabolism of naproxen from the pur-

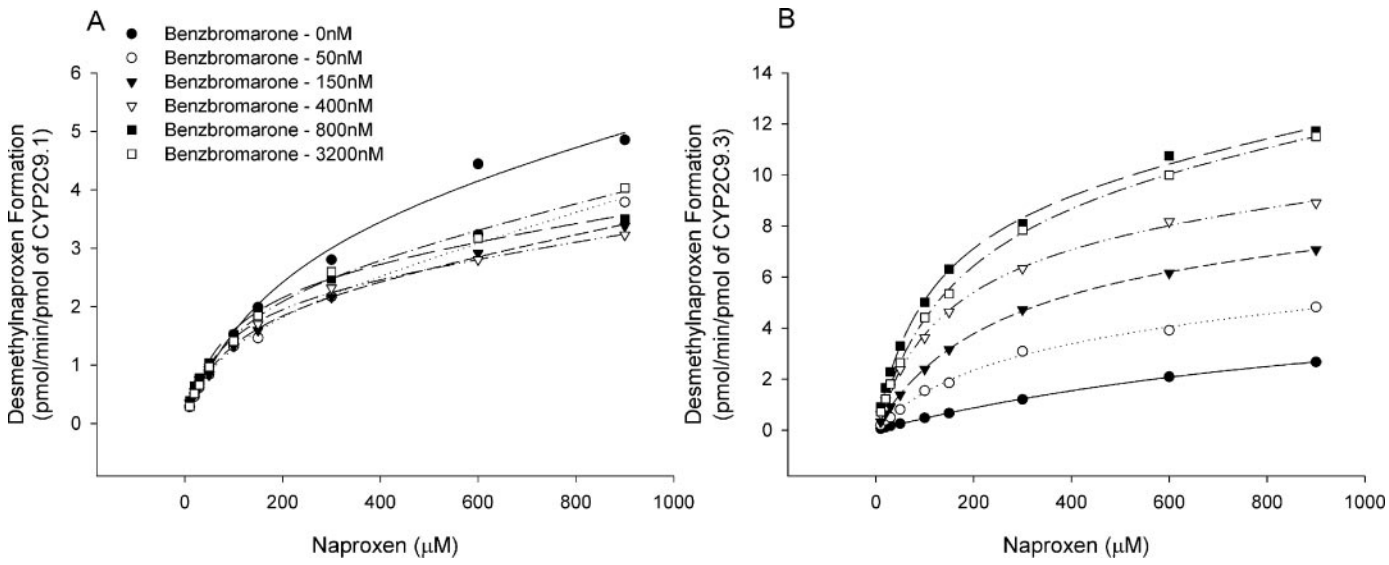

FIG. 4. Two-site model nonlinear regression fit (eq. 1) of the data for BZBR inhibition of CYP2C9.1 (A)- and activation of CYP2C9.3 (B)-mediated naproxen demethylation. Data points represent mean of duplicate determinations. Symbol explanations are the same for both A and B.

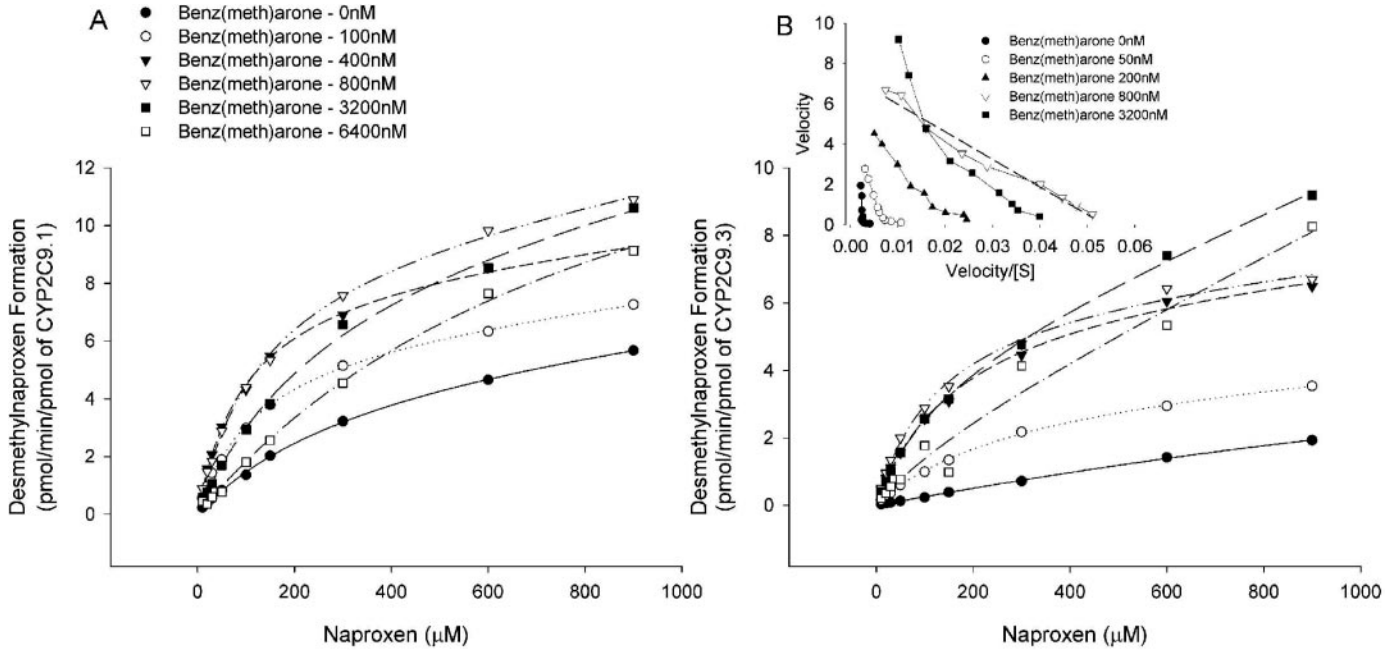

FIG. 5. Two-site model nonlinear regression fit (eq. 1) of the data for benz(meth)arone activation of CYP2C9.1 (A)- and CYP2C9.3 (B)-mediated naproxen demethylation. Data points represent mean of duplicate determinations. Symbol explanations are the same for both A and B. Inset shows Eadie-Hofstee plots for (*S*)-naproxen in the presence of benz(meth)arone using CYP2C9.3.

ported high-K_m/high-V_m (linear) portion of the process, as noted by the apparent switching of the kinetic profile from the expected biphasic profile of naproxen demethylation to a more hyperbolic profile. Surprisingly, an opposite effect of BZBR was noted when it was coincubated with naproxen in CYP2C9.3, in that enzyme activation was observed. As noted with CYP2C9.1, at higher concentrations of BZBR, the naproxen kinetic profile gradually changed from biphasic to more hyperbolic in nature in CYP2C9.3. The kinetic parameter estimates for naproxen demethylation by CYP2C9.1 and CYP2C9.3 in the presence of BZBR were obtained by using biphasic competitive inhibition ($R^2 = 0.94$) and biphasic activation models ($R^2 = 0.99$), respectively (Table 1).

Coincubation of naproxen with the dimethyl analog, benz(meth)arone, resulted in a differing effect from that noted with BZBR, as benz(meth)arone activated naproxen demethylation by the CYP2C9.1 enzyme (Fig. 5A). With increasing concentrations of benz(meth)arone, up to 400 nM, the kinetic profile of naproxen demethylation changed from biphasic to hyperbolic. Further increases in benz(meth)arone concentration (up to 1600 nM) appeared to reverse this effect and alter the kinetic profile back to biphasic in nature. At concentrations above 3200 nM, benz(meth)arone produced less activation at lower substrate concentrations, altering the kinetic profile to become hyperbolic again, with a large increase in K_m. Thus, the type of kinetic profile observed was effector concentration-dependent. In CYP2C9.3, benz(meth)arone also activated the metabolism of naproxen, altering the kinetics from a biphasic profile to a more

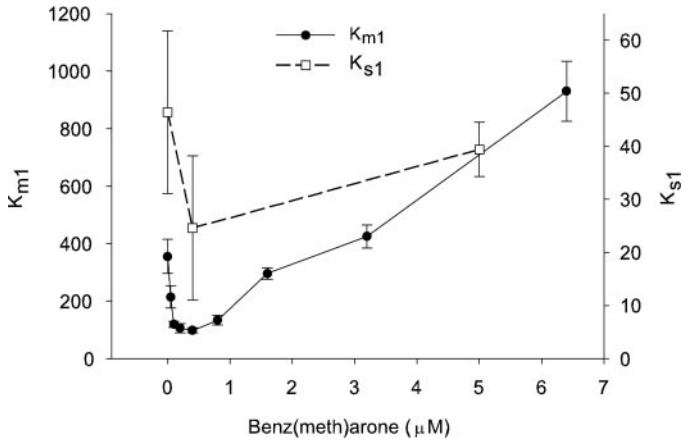

FIG. 6. Changes in the K_{m1} and K_{S1} values obtained by two-site nonlinear regression fit (eqs. 1 and 5) of CYP2C9.1-mediated naproxen demethylation versus benz(meth)arone concentration. Bars shown are standard errors of the parameters obtained by nonlinear regression fit.

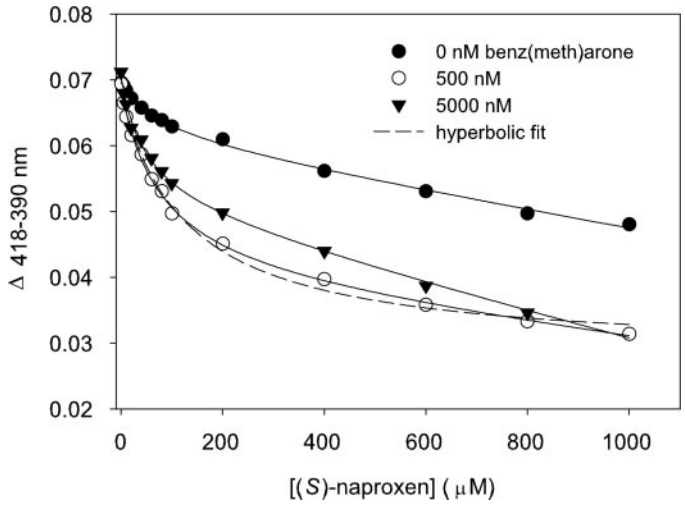

FIG. 7. Effect of naproxen on the heme iron spin equilibrium of CYP2C9.1. Lines represent fits to a two-site binding model (eq. 5), which was used to determine K_S values. A fit to a hyperbolic model is included for comparison at equimolar concentrations of enzyme and heteroactivator benz(meth)arone (dashed line).

hyperbolic profile at concentrations of benz(meth)arone up to 800 nM (Fig. 5B). Above 800 nM benz(meth)arone, the kinetic profile of naproxen metabolism again changed back from hyperbolic to biphasic, as was noted in CYP2C9.1. At the highest concentration of 6400 nM, less activation was observed at low substrate concentrations. These benz(meth)arone concentration-dependent changes in kinetic profiles are also depicted in an Eadie-Hofstee transform for clarity in Fig. 5B (inset). The data for CYP2C9.1- and CYP2C9.3-mediated naproxen demethylation in the presence of benz(meth)arone were fit ($R^2 = 0.97$ and 0.98, respectively) to an equation describing biphasic activation kinetics (eq. 3), and the parameter estimates are presented in Table 1. Based on parameter estimates of these fits, benz(meth)arone had little effect on K_m in either CYP2C9.1 or CYP2C9.3 as noted by the α values of 1.2 and 0.98, respectively. When each curve was fitted alone, there was a significant decrease in the K_{m1} from 356 to 98 μM at concentrations up to 400 nM benz(meth)arone. Also, with the change in kinetic profile, the K_{m1} values again increased from 98 μM in the presence of 400 nM benz(meth)arone to 930 μM with 6400 nM benz(meth)arone (Fig. 6). V_m changed notably, as suggested by the β parameter estimates of 2.3 and 6.8 in CYP2C9.1 and CYP2C9.3, respectively.

Equilibrium Substrate Binding. The spectral properties of the CYP2C9 heme were monitored in response to naproxen binding to determine whether the benz(meth)arone heteroactivator could alter naproxen binding in a concentration-dependent manner. Titration of naproxen into a mixture of CYP2C9.1/CPR/cytochrome b_5 enzymes similar to that used in enzyme incubations produced biphasic changes in the heme absorbance, thus suggesting that multiple binding events were detectable (Fig. 7). Upon addition of low levels of the benz(meth)arone effector, the spectral dissociation constant (K_S) of naproxen binding to the saturable, low-K_S site decreased modestly from 46.4 to 24.6 μM and increased back to 39.4 μM under high concentrations of the effector (Fig. 6). A similar profile of change in K_S values was obtained for the 2C9.3 enzyme (data not shown). K_S values for naproxen binding to the K_{S2} site could not be accurately determined because the estimated values (>2000–3000 μM) lie above the solubility of naproxen in aqueous buffer. However, the value for K_{S2} is also predicted to decrease with increasing levels of heteroactivator. In fact, it is evident in Fig. 7 that at intermediate effector concentrations, the binding profile becomes more hyperbolic and the two binding events are less distinguishable as demonstrated by the fit to a rectangular hyperbola (Fig. 7, dashed line).

Another observation was that the total signal change induced by naproxen was significantly enhanced in the presence of the effector benz(meth)arone (Fig. 7). Since the degree of change in heme iron spin state is thought to be associated with the ability of a ligand to displace a water ligand from the distal face of the heme, this could indicate the change in proximity of naproxen(s) to the heme in a qualitative manner. Occupation of the saturable, low K_{S1} site by naproxen in the presence of 500 nM benz(meth)arone produced a 272% increase in spectroscopic signal versus the absence of effector based on B_{max1} values. The second binding event, measured as the percentage signal change between 1000 μM naproxen and B_{max1}, decreased to 80% compared with 281% when effector was absent. In addition, both concentrations of effector used were less capable of converting a significant fraction of the enzyme to the high-spin state in the absence of naproxen, suggesting that it prefers to bind away from the heme even under saturating concentrations.

The effect of desethylamiodarone on CYP2C9 spectra was also tested to ascertain whether it bound largely through protein contacts or whether coordination to the heme iron was involved. No heme coordination (also known as type II interaction) was evident in difference spectra. Instead, a type I binding interaction was identified by an increasing high-spin peak at 385 nm and a decreasing low-spin trough at 418 nm, signifying the transition to a high-spin, penta-coordinate heme.

Ligand Docking. Molecular modeling was also used to gain insight as to why the amiodarone analogs display such varying effects on naproxen metabolism (Table 2). Docking was used to generate the most plausible binding conformations of all ligands. As a control, (*S*)-flurbiprofen, which was the ligand cocrystallized in the CYP2C9 enzyme structure used, docked in the same position as published in the original structure report (Wester et al., 2004). All top scoring conformations of (*S*)-naproxen placed it in the same orientation as flurbiprofen, with carboxylate interactions at the R108 and N204 sidechains and the site of metabolism closest to the heme moiety (Fig. 8). The protonation state of the substrate, remarkably, did not affect these results.

Likewise, docking studies predicted the sites of metabolism of amiodarone, BZBR (benzofuran), and, benz(meth)arone (phenol and benzofuran rings). All conformations of amiodarone docked with the amine group closest to the heme positioning it for *N*-dealkylation,

TABLE 2

Docking scores of (S)-naproxen and benzbromarone effectors and resulting changes caused by simultaneous binding

Ligand(s)	GlideScore[a]		Distance of Naproxen Methoxy Protons from Heme Iron[b]
	R108 Site[c]	F476 Site[c]	
			Å
Naproxen	−8.35		5.71
Two naproxens	−8.97	−5.32	4.78
Benz(meth)arone		−7.31	
Benzbromarone	−8.19		
Benz(meth)arone plus naproxen	−7.31 (naproxen)	−7.62 (benz(meth)arone)	5.10
	−6.50 (benz(meth)arone)	−7.41 (naproxen)	
Benzbromarone plus naproxen	−9.10 (naproxen)	−6.97 (benzbromarone)	4.77
	−6.58 (benzbromarone)	−6.97 (naproxen)	

[a] Top docking scores obtained from Glide as described under *Materials and Methods*; more negative values reflect higher binding affinity.
[b] Average taken from top scoring conformation of naproxen at the R108 site; naproxen was not favored to bind with its metabolized position near the heme in the F476 site.
[c] Location of the two binding regions identified by docking. The R108 site places the substrate naproxen nearest the heme for oxidation. When a second naproxen molecule or an effector is included, the corresponding effects on the affinity of each ligand can be calculated.

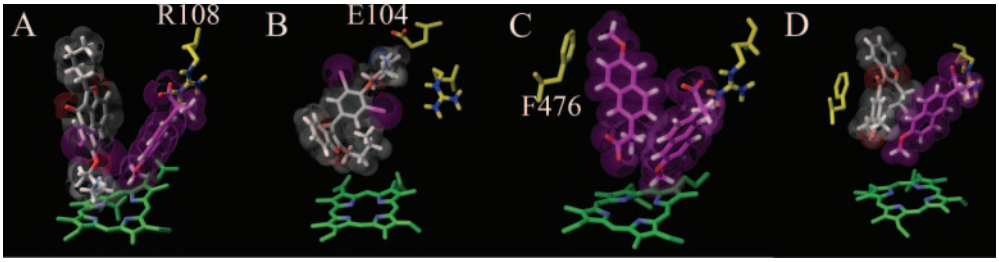

FIG. 8. Docking of naproxen and analogs of amiodarone; amiodarone docked in the presence of naproxen (magenta), which is predicted to bind to R108 with its carboxylate group (A), desethylamiodarone docked with its dealkylated amine oriented away from the heme and interacting with E104 (B), two naproxen molecules shown with the predicted effector binding site near F476 (C), naproxen (magenta) and benz(meth)arone (D).

whereas three of the top four scoring conformations of its desethyl metabolite were oriented in the reverse direction, so that the amine donated an H-bond to E104 (Fig. 8). Protonating the secondary amine of desethylamiodarone further increased the number of conformations (top seven scores) bound opposite to that of amiodarone. The negatively charged BZBR docked with its deprotonated phenol oxygen near the sidechain of R108 to form an ionic interaction and placing the benzofuran over the heme in the seven top ranking conformations. In contrast, 5 of 10 conformations of benz(meth)arone were flipped 180° versus BZBR because they were predicted to bind with the phenol ring over the heme, but in each case one of the aromatic rings was interacting with F476, leaving the binding site at R108 available. The fact that BZBR is charged at physiological pH, and benz(meth)arone is not, may contribute to the differences as evidenced by the preferential positioning of BZBR at the cationic naproxen binding site.

BZBR and benz(meth)arone were also docked in the presence of naproxen since these compounds altered the kinetic profile of naproxen. The orientations of BZBR and benz(meth)arone were restricted to basically two types, if slight bond rotamers were ignored. The two conformations by which the aromatic ring system bound near the sidechain of F476 differed. Hence, substrates were nearest to the I-helix, whereas activators were positioned between naproxen and substrate recognition site 6 (Gotoh, 1992). Only small differences in scores between the two possible ring orientations of BZBR and benz(meth)arone (0.22 and 0.40, respectively) were found. Situations in which naproxen binds to the effector site (high-K_m naproxen site) and effector binds to the naproxen site (low-K_m naproxen site) were also tested. Overall, naproxen was predicted to bind more avidly to the R108 site, even with effector present (i.e., putative low-K_m naproxen site). When a second naproxen molecule was docked, its top five scoring conformations were not oriented in a position where they would be likely to undergo metabolism at the methoxy group. Furthermore, the second naproxen molecule binding to the effector site had the lowest predicted affinity in the entire study, suggesting that the effector site is most likely the high-K_m naproxen binding site (Fig. 8). When CYP2C9 was occupied with naproxen, both BZBR and benz(meth)arone were favored to bind to the effector site.

Discussion

Knowledge of the impact of atypical kinetic phenomena and genetic polymorphisms on the drug-drug interaction potential of compounds is important in accurately making drug interaction predictions from both in vitro and in vivo data. The current studies were designed to evaluate the effects of a series of structurally related CYP2C9 effectors (amiodarone analogs) on the turnover of a prototypic substrate exhibiting atypical kinetics (naproxen) in CYP2C9.3 and wild-type CYP2C9. Interestingly, dramatically different results were noted. Each of the four amiodarone analogs studied produced unique effects on kinetic metabolism profiles that were both concentration- and genotype-dependent (Fig. 1). Further examination using equilibrium binding and docking studies suggests that CYP2C9 effectors like the amiodarone analogs may exhibit multiple binding orientations, may bind within the enzyme active site simultaneously with the substrate, and can alter the kinetic profile for naproxen turnover in a genotype-dependent fashion.

Amiodarone is a clinically important antiarrhythmic agent and has been observed to inhibit CYP2C9-mediated warfarin metabolism both in vivo and in vitro (O'Reilly et al., 1987; Nolan et al., 1989; Heimark et al., 1992; Hirmerova et al., 2003), but activation of 7-methoxyfluorocoumarin metabolism also has been observed, thus suggesting that substrate-dependent actions of amiodarone may occur (Egnell et al., 2003). Desethylamiodarone (the deethylation metabolite) is an even more potent inhibitor of CYP2C9-mediated metabolism of warfarin than the parent compound (Ohyama et al., 2000; Naganuma et al., 2001). BZBR also possesses a benzofuran primary structure like that of amiodarone but is substantially smaller in size because of the bromine substitutions, the ethyl group at C2, and the absence of the tertiary amino group that is attached to the phenolic oxygen of amiodarone. Benz(meth)arone has methyl groups substituted for the bromines, rendering the compound much smaller in size and less

acidic. This compound has also been demonstrated to be a potent in vitro inhibitor of warfarin metabolism by CYP2C9 (Locuson et al., 2004).

Regardless of genotype, amiodarone activated naproxen metabolism at low concentrations and produced weak inhibition at higher concentrations (Fig. 2). Amiodarone had no effect on the kinetic profile of naproxen demethylation, irrespective of the studied amiodarone concentration. This activation of naproxen demethylation is similar to that observed by McGinnity et al. (2005) using concentrations from 2.5 – 1000 μM and analogous to the activation of 7-methoxyfluorocoumarin by amiodarone previously reported (Egnell et al., 2003). Though we also observed activation with amiodarone, in the current study a weak inhibition was noted at amiodarone concentrations above 250 μM in both CYP2C9.1 and CYP2C9.3. These differences in study results may be due to differences in the source of the CPR enzyme, as is discussed in more detail below regarding the results with benzbromarone.

Desethylamiodarone was a potent inhibitor of naproxen demethylation in both CYP2C9.1 (K_i = 4.3 μM) and CYP2C9.3. Similar to amiodarone, desethylamiodarone did not alter the kinetic profile observed in the demethylation of naproxen. This potent inhibition of CYP2C9 is similar to that reported by Ohyama et al. (2000), using warfarin as a probe substrate of CYP2C9. These investigators studied the inhibitory potential of both amiodarone and desethylamiodarone on CYP2C9-mediated warfarin 7-hydroxylation and observed that desethylamiodarone is a much more potent inhibitor of this process (K_i = 2.3 μM) than amiodarone (K_i = 94.6 μM). However, these investigators did not evaluate whether genotype-dependent differences existed. Our results suggest that in contrast to our findings with amiodarone (inhibition of CYP2C9.3 ~8-fold weaker than with CYP2C9.1), desethylamiodarone appears to inhibit the metabolism of naproxen about equally in each enzyme.

It is striking that amiodarone and its desalkyl metabolite produce such different effects, given their similarity. Initially, we postulated that the inhibitory action of desethylamiodarone originated from its amine, which, being less hindered than the parent compound, may coordinate to the heme iron. Known as type II binding, these interactions are relatively strong for pyridine- and imidazole-containing compounds, but also occur with primary and secondary amines. Difference spectroscopy of CYP2C9 during titration of desesthylamiodarone, however, revealed a type I binding interaction suggesting that the favored conformation(s) of CYP2C9-bound desethylamiodarone destabilizes the low-spin state rather than stabilizing it (data not shown). Moreover, docking studies demonstrated preference for the amine to bind at E104, placing the large iodine atoms closer to the I-helix, where naproxen is predicted to bind (Fig. 8). This would explain why, unlike amiodarone, desethylamiodarone is an inhibitor of naproxen metabolism at all concentrations.

Previously, Hummel et al. (2005) reported a genotype-dependent effect of BZBR on flurbiprofen 4′-hydroxylation in CYP2C9.1 versus CYP2C9.3. BZBR inhibited flurbiprofen 4′-hydroxylation by CYP2C9.1, but in contrast, BZBR activated this same reaction when studied with the variant CYP2C9.3 allele. Yet, this study evaluated a hyperbolic (typical) kinetics substrate (flurbiprofen) that is thought to bind in only one productive orientation within the CYP2C9 active site. The use of a substrate that exhibits atypical kinetics (naproxen) and is thought to bind simultaneously in two productive orientations may exhibit differences in the effects of BZBR on substrate metabolism. Similar to the results observed with coincubation of flurbiprofen and BZBR (Hummel et al., 2005), naproxen demethylation was inhibited by BZBR when metabolized by CYP2C9.1 but was activated by BZBR in the CYP2C9.3 variant. This contrasts with the recent results of McGinnity et al. (2005), which demonstrated that BZBR activates naproxen demethylation in recombinant CYP2C9.1. The reason(s) for this difference is unclear, but in the current study, when human reductase was used in place of rat reductase in the incubation, activation and normalization of naproxen demethylation was observed in CYP2C9.1 (data not shown), suggesting that protein-protein interactions may also affect the type of kinetic interaction observed. This is analogous to the change in pyrene kinetic profile observed depending on whether cytochrome b_5 is present in the incubation (Jushchyshyn et al., 2005). Full exploration of this interesting phenomenon of kinetic profiles controlled by protein-protein interactions is beyond the scope of the current study but is a subject of current research in our laboratory.

Interestingly, in both CYP2C9.1 and CYP2C9.3, BZBR normalized the kinetics of naproxen demethylation from biphasic to hyperbolic, but the mechanism(s) by which this normalization occurs appears to differ in the wild-type and variant CYP2C9 enzyme. In CYP2C9.1, BZBR normalized the kinetics of naproxen demethylation by inhibition via the purported higher-K_m site only, but normalization of kinetics in CYP2C9.3 was accomplished through apparent activation of naproxen metabolism via the purported low-K_m binding region, the high-K_m binding region, or both. Together, these results suggest that BZBR may adopt multiple binding orientations (see below), and the preferred binding mode of BZBR is genotype-dependent.

Finally, benz(meth)arone was a potent activator of naproxen demethylation both in CYP2C9.1 and CYP2C9.3. Interestingly, this interaction normalized naproxen kinetics, resulting in a switch from a biphasic to a hyperbolic profile with increasing concentrations of benz(meth)arone up to 800 nM. These results are analogous to those observed previously with dapsone activation of naproxen demethylation in the CYP2C9.1 enzyme (Hummel et al., 2004). However, when the concentrations of benz(meth)arone were increased to 6400 nM, the kinetic profile reverted back to an apparent biphasic or possibly very high-K_m hyperbolic shape, a result not previously observed with dapsone activation. This reversion to a biphasic kinetic profile was even more pronounced in CYP2C9.3.

Two hypotheses may explain these observations, which probably result from a population of enzyme-ligand complexes. The first is that more than two ligands are capable of binding to a CYP2C9. For instance, a P450-naproxen-naproxen-effector complex becomes a P450-naproxen-effector complex as effector is increased. Or, a P450-naproxen-effector complex becomes P450-naproxen-effector-effector. A simpler explanation involves multiple binding modes for BZBR and benz(meth)arone. It is possible that at lower concentrations (<800 nM), benz(meth)arone occupies the naproxen binding site in CYP2C9 that is responsible for the high-K_m/high-V_m portion of the kinetic profile and activates metabolism of naproxen largely by steric effects that increase reaction velocity. This is supported by the decreased naproxen-heme distances (Table 2) and the large changes in the ability to alter spin state (Fig. 7). At higher effector concentrations, binding of effector to the low K_m/high V_m may compete with naproxen, but even higher velocities for naproxen oxidation are possible from the P450-naproxen-effector complex because the effector site is closer to being saturated with effector; however, higher naproxen concentrations may be required to form this intermediate at high effector concentrations. Docking studies agree with the above hypothesis and suggest distinct subsites in the CYP2C9 active site. The favored binding conformation of naproxen resembles that of flurbiprofen captured crystallographically; thus, it is proposed that the low-K_m site for naproxen lies between the I-helix and the effector binding site (high-K_m site near F476), which, when occupied, limits naproxen to remain in close proximity to the heme cofactor.

In conclusion, amiodarone and its analogs exhibit differential effects on the metabolism as well as kinetics of naproxen demethylation. Binding of these effector molecules in multiple orientations within the CYP2C9 active site may account for some of these differential and concentration-dependent effects.

Acknowledgments. We thank the University of Minnesota Supercomputing Institute for technical assistance.

References

Egnell AC, Eriksson C, Albertson N, Houston B, and Boyer S (2003) Generation and evaluation of a CYP2C9 heteroactivation pharmacophore. *J Pharmacol Exp Ther* **307:**878–887.

Gotoh O (1992) Substrate recognition sites in cytochrome P450 family 2 (CYP2) proteins inferred from comparative analyses of amino acid and coding nucleotide sequences. *J Biol Chem* **267:**83–90.

Hanna IH, Teiber JF, Kokones KL, and Hollenberg PF (1998) Role of the alanine at position 363 of cytochrome P450 2B2 in influencing the NADPH- and hydroperoxide-supported activities. *Arch Biochem Biophys* **350:**324–332.

Heimark LD, Wienkers L, Kunze K, Gibaldi M, Eddy AC, Trager WF, O'Reilly RA, and Goulart DA (1992) The mechanism of the interaction between amiodarone and warfarin in humans. *Clin Pharmacol Ther* **51:**398–407.

Higashi MK, Veenstra DL, Kondo LM, Wittkowsky AK, Srinouanprachanh SL, Farin FM, and Rettie AE (2002) Association between CYP2C9 genetic variants and anticoagulation-related outcomes during warfarin therapy. *J Am Med Assoc* **287:**1690–1698.

Hirmerova J, Suchy D, and Madr T (2003) [Long-term drug interaction of warfarin with amiodarone]. *Cas Lek Cesk* **142:**39–42.

Hummel MA, Dickmann LJ, Rettie AE, Haining RL, and Tracy TS (2004) Differential activation of CYP2C9 variants by dapsone. *Biochem Pharmacol* **67:**1831–1841.

Hummel MA, Locuson CW, Gannett PM, Rock DA, Mosher CM, Rettie AE, and Tracy TS (2005) CYP2C9 genotype-dependent effects on in vitro drug-drug interactions: switching of benzbromarone effect from inhibition to activation in the CYP2C9.3 variant. *Mol Pharmacol* **68:**644–651.

Jushchyshyn MI, Hutzler JM, Schrag ML, and Wienkers LC (2005) Catalytic turnover of pyrene by CYP3A4: evidence that cytochrome B5 directly induces positive cooperativity. *Arch Biochem Biophys* **438:**21–28.

Korzekwa KR, Krishnamachary N, Shou M, Ogai A, Parise RA, Rettie AE, Gonzalez FJ, and Tracy TS (1998) Evaluation of atypical cytochrome P450 kinetics with two-substrate models: evidence that multiple substrates can simultaneously bind to cytochrome P450 active sites. *Biochemistry* **37:**4137–4147.

Lee CR, Goldstein JA, and Pieper JA (2002) Cytochrome P450 2C9 polymorphisms: a comprehensive review of the in-vitro and human data. *Pharmacogenetics* **12:**251–263.

Locuson CW, Gannett PM, and Tracy TS (2006) Heteroactivator effects on the coupling and spin state equilibrium of CYP2C9. *Arch Biochem Biophys* **449:**115–129.

Locuson CW, Rock DA, and Jones JP (2004) Quantitative binding models for CYP2C9 based on benzbromarone analogues. *Biochemistry* **43:**6948–6958.

McGinnity DF, Tucker J, Trigg S, and Riley RJ (2005) Prediction of CYP2C9-mediated drug-drug interactions: a comparison using data from recombinant enzymes and human hepatocytes. *Drug Metab Dispos* **33:**1700–1707.

Naganuma M, Shiga T, Nishikata K, Tsuchiya T, Kasanuki H, and Fujii E (2001) Role of desethylamiodarone in the anticoagulant effect of concurrent amiodarone and warfarin therapy. *J Cardiovasc Pharmacol Ther* **6:**363–367.

Nolan PE Jr, Marcus FI, Hoyer GL, Bliss M, and Gear K (1989) Pharmacokinetic interaction between intravenous phenytoin and amiodarone in healthy volunteers. *Clin Pharmacol Ther* **46:**43–50.

Ohyama K, Nakajima M, Suzuki M, Shimada N, Yamazaki H, and Yokoi T (2000) Inhibitory effects of amiodarone and Its N-deethylated metabolite on human cytochrome P450 activities: prediction of in vivo drug interactions. *Br J Clin Pharmacol* **49:**244–253.

O'Reilly RA, Trager WF, Rettie AE, and Goulart DA (1987) Interaction of amiodarone with racemic warfarin and its separated enantiomorphs in humans. *Clin Pharmacol Ther* **42:**290–294.

Rendic S and Di Carlo FJ (1997) Human cytochrome P450 enzymes: a status report summarizing their reactions, substrates, inducers, and inhibitors. *Drug Metab Rev* **29:**413–580.

Takanashi K, Tainaka H, Kobayashi K, Yasumori T, Hosakawa M, and Chiba K (2000) CYP2C9 Ile359 and Leu359 variants: enzyme kinetic study with seven substrates. *Pharmacogenetics* **10:**95–104.

Tate SK, Depondt C, Sisodiya SM, Cavalleri GL, Schorge S, Soranzo N, Thom M, Sen A, Shorvon SD, Sander JW, et al. (2005) Genetic predictors of the maximum doses patients receive during clinical use of the anti-epileptic drugs carbamazepine and phenytoin. *Proc Natl Acad Sci USA* **102:**5507–5512.

Tracy TS, Marra C, Wrighton SA, Gonzalez FJ, and Korzekwa KR (1997) Involvement of multiple cytochrome P450 isoforms in naproxen O-demethylation. *Eur J Clin Pharmacol* **52:**293–298.

Wester MR, Yano JK, Schoch GA, Yang C, Griffin KJ, Stout CD, and Johnson EF (2004) The structure of human cytochrome P450 2C9 complexed with flurbiprofen at 2.0-A resolution. *J Biol Chem* **279:**35630–35637.

Address correspondence to: Dr. Timothy S. Tracy, Dept. of Experimental and Clinical Pharmacology, College of Pharmacy, University of Minnesota, 308 Harvard St. SE, Minneapolis, MN 55455. E-mail: tracy017@umn.edu